Applied Catalysis B: Environmental 92 (2009) 100–113

Contents lists available at ScienceDirect

Applied Catalysis B: Environmental

journal homepage: www.elsevier.com/locate/apcatb

Dibenzothiophene hydrodesulfurization over cobalt phosphide catalysts prepared through a new synthetic approach: Effect of the support

J.A. Cecilia, A. Infantes-Molina, E. Rodríguez-Castellón, A. Jiménez-López *

Departamento de Química Inorgánica, Cristalografía y Mineralogía (Unidad Asociada al ICP-CSIC), Facultad de Ciencias, Universidad de Málaga, Campus de Teatinos, 29071 Málaga, Spain

ARTICLE INFO

Article history:
Received 12 May 2009
Received in revised form 13 July 2009
Accepted 20 July 2009
Available online 25 July 2009

Keywords:
Mesoporous MCM-41
Silica
Alumina
MCM-Zr
Cobalt phosphide
Dibenzothiophene
HDS

ABSTRACT

Several cobalt phosphide catalysts, with a cobalt loading of 10 wt%, were prepared by means of temperature-programmed reduction (TPR) of cobalt(II) hydrogenphosphite ($Co(HPO_3H)_2$) supported on different carriers: two mesoporous supports, MCM-41 and zirconium doped MCM-41 (MCM-Zr), as well as two commercial supports, SiO_2 (Cab-osil) and γ-Al_2O_3. The purpose of this work is to study the role of the support on the formation of CoP or Co_2P and the analysis of the catalytic activity in the hydrodesulfurization (HDS) of dibenzothiophene (DBT). It is the CoP phase which is favoured on these catalysts under the given experimental conditions, except for that supported on γ-Al_2O_3 (CoP-10 (Al)), which only displays the diffraction lines of the Co_2P phase after the reduction process. The interaction support–precursor salt seems to determine which of the phases is formed. The catalytic results showed that this family of catalysts obtained high DBT conversion values at high temperatures, mainly via the direct desulfurization (DDS) route, i.e., yielding biphenyl (BP) as majority product and attaining turnover frequency (TOF) values of 0.87×10^{-3} s^{-1}. The stability with time on stream showed that the silica (Cab-osil) supported catalyst, CoP-10 (Cab), was highly stable with time on stream (48 h) with conversion values close to 100% and with a performance similar to that of Ni_2P catalysts and better than other cobalt phosphide catalysts reported in the literature. In contrast, the CoP-10 (Zr) and CoP-10 (Si) samples decrease in activity after 16 h on stream, although their conversions are between 65% and 70% after 48 h on stream. Finally, the CoP-10 (Al) catalyst provided lower conversion values and underwent deactivation with time on stream due to the low activity of the Co_2P compound formed on this sample. Furthermore, the analysis of the spent catalyst showed the presence of sulfur on the surface, assigned to the formation of phosphosulfide species.

1. Introduction

A cleaner environment requirement has led to government regulations to produce and use fuels with lower sulfur, nitrogen and aromatic content. The Environment Protection Agency (EPA) has legislated a reduction of sulfur content from 500 to 15 parts per million by weight (wppm) during the period 2007–2010, and the laws will be more restrictive at the beginning of 2011 when the sulfur content must be reduced to less than 10 wppm [1]. The restrictive regulations in the European Union are also similar, and a maximum sulfur content of 10 wppm is forecast. Moreover, the reduction in petroleum reserves has provoked the use of feedstocks of lower quality (typical crude contains 1.5% sulfur). Hence a renewed interest has arisen to develop highly active catalysts for sulfur removal in hydrotreating reactions. The sulfur compounds present in feedstock are mostly refractory molecules from the thiophene or dibenzothiophene family that can also possess alkyl groups, which hinder the removal of sulfur [2]. Therefore, a worldwide search for improved catalysts has been undertaken.

One of the research areas is to improve the traditional sulfide catalysts, which are mainly based on alumina supported molybdenum or tungsten sulfides, where cobalt or nickel is present in the form of a so-called "Co-Mo-S" or "Ni-No-S" promoter phase at the edges of the molybdenum or tungsten sulfided crystals. These promoters modify the particle morphologies and increase the catalyst acidity [3,4]. Phosphorus has also been added as a secondary promoter to modify the properties of the support, as well as indirectly acting on the active phase [5], thus increasing the heteroatom removal activity, and improving the mechanical and thermal stability [6].

New approaches have also been taken by using transition metal carbides [7,8], nitrides [8,9], borides [10] and above all phosphides [11,12]. All of them show high activity in both hydrodesulfurization (HDS) and hydrodenitrification (HDN) reactions. The main

* Corresponding author. Tel.: +34 952131876; fax: +34 952137534.
E-mail address: ajimenezl@uma.es (A. Jiménez-López).

0926-3373/$ – see front matter © 2009 Elsevier B.V. All rights reserved.
doi:10.1016/j.apcatb.2009.07.017

drawback of carbides and nitrides is their instability in the presence of H_2S (the product obtained during the HDS reaction), whereby they undergo deactivation [13]. Unlike the latter, transition metal phosphides are found to be active and stable under HDS conditions. The initial studies of phosphides were carried out in hydrogenation reactions [14] and subsequently their applications in HDS and HDN reactions were realised [15]. Following this, a great number of studies were devoted to the synthesis and hydrotreating activity of phosphide based catalysts. Hence, a number of transition metal phosphides have been prepared: Ni_2P [11,12,16], CoP [17,18], Co_2P [19], MoP [20], WP [19] as well as mixed phosphides such as CoMoP [21], NiMoP [22], $Co_xNi_{2-x}P$ [23]. Regarding the phosphide family, the Ni_2P phase has been fully documented as being the most active [18] and has consequently been the subject of the most detailed studies. Authors in this area of research have demonstrated, by different experimental techniques that during the catalytic run a superficial incorporation of sulfur takes place, coating the phosphide particles with the formation of a superficial phosphosulfide phase. This intermediate phase is the active component of the transition metal phosphides in HDS reactions [24,25].

There has been very little research on the HDS properties of cobalt phosphide catalysts, as the activity of this phase is reported to be lower than that of Ni_2P, although better than other phosphides [18]. Also, as is the case with nickel phosphides, cobalt phosphides exist with different stoichiometries: CoP, Co_2P and CoP_2. The CoP structure exhibits most activity and stability [17] in the HDS reaction. The formation of the desired cobalt phosphide depends on two factors, the P/Co ratio and the interaction phosphorous–support. Bussell and co-workers [17] have recently reported that high P/Co ratios (>2) lead to the formation of CoP, whereas low P/Co ratios (<0.5) favour the formation of Co_2P. The precursor–support interaction is directly correlated to the support acidity. Thus, it has been reported that the phosphine (PH_3) formed during reduction reacts with metallic particles, which are first reduced to form the corresponding phosphide [26]. Therefore, the phosphorous–support interaction determines the PH_3 liberation and/or the formation of the corresponding phosphide. With respect to this, Oyama et al. [11] found greater phosphine and water loss when less acidic supports were used and the support–precursor interaction is lesser. Also of consequence are the geometric and electronic properties of the active phase obtained.

The role of the support has been studied in both traditional sulfide [27] and nickel phosphide catalysts [28]. However, its effect on cobalt phosphide systems has hardly been considered. In general, silica has been the most frequently used support for phosphide catalysts [18] because the support–precursor interaction is weak due to the low acidity of the silica. Besides silica, various other supports have been tested, such as the mesoporous silica MCM-41 [29] and SBA-15 [30]. γ-Al_2O_3 has also been considered as the best carrier for traditional sulfided catalysts. However, when it was used as support of transition phosphides, it strongly interacted with the precursors to form $AlPO_4$ [26,28], requiring a higher reduction temperature.

In this paper, we describe the formation and catalytic properties of cobalt phosphide catalysts in the DBT HDS reaction. Traditionally, this phosphide has been synthesized by impregnation of the support with $(NH_4)_2HPO_4$ or $NH_4H_2PO_4$ and $Co(NO_3)_2$, and the cobalt phosphide particles being formed after calcination and H_2 thermoprogrammed reduction [18]. In this work, a new method [31] that combines cobalt hydroxide, $Co(OH)_2$, and phosphorous acid, H_2PO_3H, that reacts to form $Co(HPO_3H)_2$, is proposed. This method has several advantages: there is no need of the calcination step of the precursors and also lower reduction temperature and hydrogen flows are required to obtain the desired active phase than those used in the literature. The catalytic results reported here are much better than those found in the literature for cobalt phosphide catalysts in the HDS reaction [18], which indicates the importance of the preparation method exposed here.

2. Experimental

2.1. Materials

The supports used in this study were traditional mesoporous silica MCM-41 [32], mesoporous silica doped with zirconium with a Si/Zr molar ratio = 5 [33], a commercial silica (Cab-osil® M-5) and a commercial γ-Al_2O_3 supplied by REPSOL. Cobalt(II) hydroxide ($Co(OH)_2$ Aldrich 95%) and phosphorous acid (H_2PO_3H Aldrich 99%) were employed to obtain the precursor $Co(HPO_3H)_2$. The chemical products utilized in the reactivity study were dibenzothiophene (Aldrich 98%) in cis-, trans-decahydronaphthaline (Sigma–Aldrich 98%). The gases employed were He (Air Liquide 99.99%), H_2 (Air Liquide 99.999%), N_2 (Air Liquide 99.9999%), NH_3 (Air Liquide 99.9%) and CO (Air Liquide 99.9%).

2.2. Preparation of catalysts

Four cobalt phosphide catalysts with a 10 wt% of cobalt supported on different supports were prepared. The supports used were the traditional mesoporous silica (MCM-41) [32]; that doped with zirconium with a Si/Zr molar ratio = 5 [33]; a commercial silica such as Cab-osil; and a commercial alumina such as γ-Al_2O_3. Phosphorus and cobalt were introduced by the incipient wetness impregnation method but using a solution of cobalt(II) dihydrogenophosphite ($Co(HPO_3H)_2$), prepared by adding the stoichiometric amounts of cobalt(II) hydroxide ($Co(OH)_2$) and phosphorous acid (H_2PO_3H) to the incipient volume. Once the cobalt(II) aqueous salt solution was added to the pelletized support (0.85–1.00 mm), it was air dried. A XRD measurement of the supports impregnated with this salt was carried out previously in order to discard the presence of undesired phases. The diffractogram did not show any peaks since this compound is totally amorphous. Finally, a temperature-programmed reduction was used to convert the phosphite into phosphide according to the method previously described [31], i.e., it was carried out in a tubular reactor, heating at linear temperature ramp (3 °C min^{-1}) in flowing hydrogen (100 ml min^{-1}) from 100 °C to the corresponding reduction temperature.

The concentration of the precursor solutions was adjusted to 10 wt% of cobalt, and they will be referred to as CoP-10 (Si), CoP-10 (Zr), CoP-10 (Cab) and CoP-10 (Al), when the supports used are MCM-41, MCM-Zr, Cab-osil and γ-Al_2O_3, respectively.

2.3. Characterization of catalysts

Powder diffraction patterns were collected on an X'Pert Pro MPD automated diffractometer equipped with a Ge(1 1 1) primary monochromator (strictly monochromatic Cu-K_α radiation) and an X'Celerator detector.

The evolved gases in the H_2-temperature-programmed reduction (TPR) experiments were sampled into a quadrupole mass spectrometer Balzer GSB 300 02 equipped with a Faraday detector, and masses 2 (H_2), 18 (H_2O), 31 (P) and 34 (PH_3) were monitored during the experiment. These signals in real time versus temperature were recorded by on-line computer.

CO chemisorption was analyzed in a Micromeritics ASAP 2010 apparatus under static volumetric conditions. Samples were reduced ex situ and transferred in inert atmosphere. Prior to measurement, samples were re-reduced in situ in H_2 at 300 °C and evacuated at 35 °C for 10 h. The chemisorption isotherm

was obtained by measuring the adsorbed amount of CO for pressures varying from 10 to 600 mmHg. After completing the initial analysis, the reversibly adsorbed gas was evacuated and the analysis repeated to determine the chemisorbed molecules only.

The textural parameters were evaluated from the nitrogen adsorption–desorption isotherms at −196 °C as determined by an automatic ASAP 2020 system from Micromeritics. Elemental chemical analysis was performed for spent catalysts with a LECO CHNS 932 analyser to determine the sulfur content present after the catalytic test.

Temperature-programmed desorption of ammonia (NH_3-TPD) was carried out to evaluate the total acidity of the catalysts. Catalyst precursors were reduced at atmospheric pressure by flowing hydrogen (100 ml min^{-1}) from room temperature to 500 °C with a heating rate of 3 °C min^{-1}. After cleaning with helium and adsorption of ammonia at 100 °C, the NH_3-TPD was performed between 100 and 550 °C with a heating rate of 10 °C min^{-1} by using a helium flow and maintained at 550 °C for 15 min. The evolved ammonia was analyzed by on-line gas chromatography (Shimadzu GC-14A) provided with a TCD.

X-ray photoelectron spectra were collected using a Physical Electronics PHI 5700 spectrometer with non-monochromatic AlK_α radiation (300 W, 15 kV, and 1486.6 eV) with a multi-channel detector. Spectra of pelletized samples were recorded in the constant pass energy mode at 29.35 eV, using a 720 μm diameter analysis area. Charge referencing was measured against adventitious carbon (C 1s at 284.8 eV). A PHI ACCESS ESCA-V6.0 F software package was used for acquisition and data analysis. A Shirley-type background was subtracted from the signals. Recorded spectra were always fitted using Gaussian–Lorentzian curves in order to determine the binding energy of the different element core levels more accurately. Reduced and spent catalysts were stored in sealed vials with an inert solvent. The sample preparation was done in a dry box under a N_2 flow, where the solvent was evaporated prior to its introduction into the analysis chamber, and directly analyzed without previous treatment.

TEM micrographs of the catalysts were obtained with a Philips CM 200 Supertwin-DX4 high resolution transmission electron microscope. Once the samples were reduced, they were kept in cyclohexane. For sample preparation, a drop of these suspensions was dispersed on a Cu grid.

2.4. Catalytic test

For the catalytic test, the hydrodesulfurization of DBT was chosen, which was performed in a high-pressure fixed-bed continuous-flow stainless steel catalytic reactor (9.1 mm in diameter, and 230 mm in length), operated in the down-flow mode. The reaction temperature was measured with an interior placed thermocouple in direct contact with the catalyst bed. The organic feed consisted of a solution of DBT (3000 ppm) in decalin that was supplied by means of a Gilson 307SC piston pump (model 10SC). For the activity tests, 0.5 g of catalyst was used (particle size 0.85–1.00 mm) and was diluted with quartz sand to 3 cm^3. Prior to the activity test, the catalysts were reduced in situ at atmospheric pressure with a H_2 flow of 100 ml min^{-1} by heating from r.t. to 500 °C at a heating rate of 3 °C min^{-1}. Catalytic activities were measured at different temperatures (300–475 °C), under 3.0 MPa of H_2, with a flow rate of 100 ml min^{-1} and with hourly space velocities (WHSV) of 32 h^{-1}. Moreover, the stabilities of the catalysts were studied at a constant temperature reaction for 48 h. The evolution of the reaction was monitored by collecting liquid samples after 60 min at the desired reaction temperature. These liquid samples were kept in sealed vials and subsequently analyzed by gas chromatography (Shimadzu GC-14B, equipped with a flame ionization detector and a capillary column, TBR-14, coupled to an automatic Shimadzu AOC-20i injector). For these catalysts, the main products of the reaction were biphenyl (BP), cyclohexylbenzene (CHB), bicyclohexyl (BCH), benzene (B) and cyclohexane (CH). For this reason, the total conversion was calculated from the ratio of converted dibenzothiophene/initial dibenzothiophene. The selectivity of the different reaction products was calculated considering BP, CHB, B and CH as the only products obtained, since only slight traces of some unknown compounds were noticeable in a few cases.

Turn over frequency values were calculated from the formula,

$$\mathrm{TOF} = \frac{F}{W}\frac{X}{M}$$

where F is the molar rate of reactant, W is the catalyst weight, X is the conversion and M is the mole of sites loaded.

3. Results and discussion

3.1. Characterization of catalysts

3.1.1. Temperature-programmed reduction of CoP-10 catalyst precursors

The formation of cobalt phosphide from the supported precursor, $Co(HPO_3H)_2$ on the different supports, was carried out by H_2-TPR method, while the gases evolved in the reduction were analyzed with a quadrupole mass spectrometer. The H_2O (m = 18) and PH_3 (m = 34) signals, which are the most pronounced ones, are plotted in Fig. 1.

The H_2O loss profiles show two main features: one loss at low temperatures (150–300 °C) and another and more complex at T >400 °C [34]. The first band could be due to both physically absorbed water and water derived from the precursor $Co(HPO_3H)_2$ salt, since it has a hygroscopic character. Further liberation of water at higher temperatures (T >400 °C) is related to the reduction processes leading to the formation of the cobalt phosphide [34]. Fig. 1 clearly shows the dependence on the support employed. While CoP-10 (Si) and CoP-10 (Cab) have intense and well defined bands, the CoP-10 (Zr) and CoP-10 (Al) samples only show a slight H_2O loss at high temperature. The first conclusion to be drawn from this plot is the low degree of reduction taking place on CoP-10 (Zr) and CoP-10 (Al), possibly due to a stronger precursor–support interaction.

With regard to the PH_3 signal, CoP-10 (Si) and CoP-10 (Cab) also show two PH_3 losses. PH_3 is evolved due to the phosphorous excess present in the precursor with regard to cobalt. Thus, a first loss (300–425 °C) can be caused by the transformation of superficially located HPO_3H^- ions interacting weakly with the support. The second loss (T >425 °C) must be related to the transformation of HPO_3H^-, which strongly interacts with the support, and both transformations are linked to the formation of CoP. On the other hand, in the case of CoP-10 (Zr) and CoP-10 (Al), hardly any phosphine loss was observed, as had occurred in the water profiles, and therefore a greater excess of non-reduced phosphorous is expected to be present on the catalyst surface, together with a lower proportion of CoP being formed.

After these TPR experiments (100–800 °C) the catalysts were analyzed by XRD (Fig. 2). In all cases, diffraction lines arising from CoP phase located at 2θ = 31.6°, 32.0°, 35.3°, 36.3°, 36.6°, 46.6°, 48.1°, 48.4°, 52.2°, 56.0° and 56.7° (PDF 00-029-0497) are present, with CoP-10 (Si) being the sample which gives the most defined diffraction lines. Contrary to this is CoP-10 (Cab), which only shows less intense and broader diffraction lines of CoP phase, suggesting a higher dispersion on the support. Diffraction lines of the Co_2P compound located at 2θ = 40.7° and 43.3° (PDF 00-032-0306) are also present in the case of CoP-10 (Zr) and CoP-10 (Al). It could be

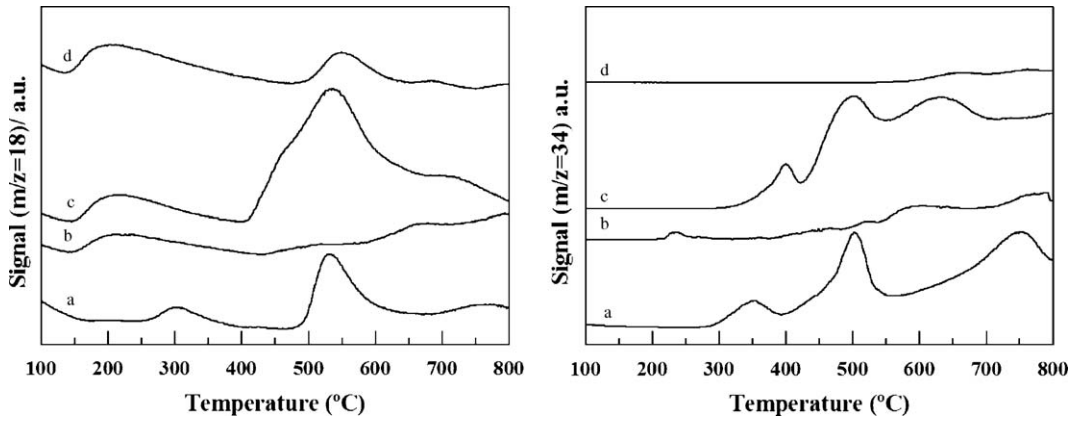

Fig. 1. Mass 18 (H_2O) and 34 (PH_3) signals from temperature-programmed reduction of samples: (a) CoP-10 (Si), (b) CoP-10 (Zr), (c) CoP-10 (Cab) and (d) CoP-10 (Al) catalysts.

said, as was seen for the Ni_2P phase [26], that the formation of CoP occurs through a sequence of intermediates, one of which would be Co_2P that subsequently reacts with PH_3 to give CoP, a phosphorous rich phase. Therefore CoP-10 (Zr) and CoP-10 (Al), which hardly liberate any PH_3, do not reduce enough hydrogenphosphite ions to form CoP in the same way that CoP-10 (Si) and CoP-10 (Cab) do.

These results are in agreement with those published by Oyama and co-workers [34], who reported that the formation of CoP is favoured when using low Co/P ratios. The precursor catalysts possess a theoretical Co/P ratio of 0.5, i.e., an excess of phosphorous is present on the samples.

3.1.2. XRD

To determine the optimal conditions for preparing these catalysts, the formation of CoP as a function of temperature was observed by XRD. Fig. 3 brings together the diffractograms obtained at different temperatures for each catalyst. Fig. 3a shows the diffractograms of CoP-10 (Si) sample at temperatures ranging from 400 to 500 °C. The diffractograms at 400 and 450 °C show that only a partial reduction of the precursor took place at low temperatures. However, the reduction is noteworthy at 500 °C where only CoP lines are distinguishable, with the main diffraction line located at $2\theta = 48.1^\circ$ (PDF 00-029-0497).

Fig. 3b depicts the diffractograms corresponding to CoP-10 (Zr) reduced at different temperatures. XRD lines arising from the presence of CoP are observable at 450 °C. The intensities of the diffraction lines are lower than those of CoP-10 (Si) sample since the presence of zirconium inside the pores leads to a stronger support–precursor interaction, as indicated from the previous study of the H_2O and PH_3 signals. From these diffractograms and TPR curves, it can be concluded that a low proportion of CoP is formed on this support and it is present as small particles.

In Fig. 3c the diffractograms of CoP-10 (Cab) reduced at different temperatures are plotted. We can see that only CoP phase is formed, although the diffraction lines are not well defined. By considering the TPR results, where a great loss of water is observed, it must be assumed that there is a considerable degree of reduction of this catalyst, being similar to that of CoP-10 (Si) sample. Nonetheless, the CoP particles formed are small enough due to their large diffraction peaks. Only the main diffraction line of the CoP phase, located at $2\theta = 48.1^\circ$, is noticeable at 450 °C.

Finally, Fig. 3d shows the diffractograms of CoP-10 (Al) sample. In all cases, the diffraction lines arising from the support at $2\theta = 37.5^\circ$ and 39.5° (PDF 01-077-0396), are present. XRD measurements show that the reduction between 500 and 550 °C leads to a single species of Co_2P, whose most intense peak is located at $2\theta = 40.5^\circ$ (PDF 00-006-0595). However, the reduction at 600 °C generates a mixture of CoP and Co_2P phases. The formation of Co_2P can be attributed to an intense interaction between phosphorous and γ-Al_2O_3, that makes the reduction process difficult. For this reason, metal-rich species (Co_2P) at low temperatures are obtained. The formation of CoP only takes place when the temperature increases.

In general the diffractograms reveal that the formation of CoP is favoured on these samples, probably due to the low Co/P ratio used. In the case of CoP-10 (Al), the precursor–support interaction is so strong that it probably requires higher temperatures to form CoP, as previously reported [35].

Given these results, we chose 500 °C as the reduction temperature prior to the catalytic reaction. This temperature is lower than that used to reduce the traditional phosphate precursor to form the cobalt phosphide phase. In this sense, temperatures of 550 °C [19], 627 °C [18] and 650 °C [17] are reported with higher hydrogen flows.

By applying the Scherrer equation to the main diffraction line of the CoP phase at $2\theta = 48.1^\circ$, the particle size was calculated. Some diffractograms do not possess a sufficiently well defined diffraction line to measure the particle size, therefore XRDs were re-run with a high resolution between $2\theta = 45^\circ$ and 51° increasing the counts number. These measurements provided particle sizes of 62 nm for CoP-10 (Si), 30 nm for CoP-10 (Zr) and 32 nm for CoP-10 (Cab), respectively. The CoP-10 (Al) sample reduced at 500 °C does not possess the diffraction lines of the CoP compound. The only phase present at this temperature is Co_2P. Application of the Scherrer equation to the main diffraction line of the Co_2P phase located at $2\theta = 40.5^\circ$ provides a particle size of 59 nm.

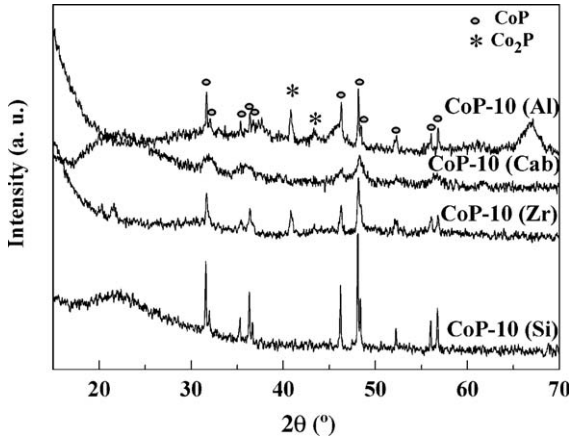

Fig. 2. XRD patterns of the catalysts after H_2-TPR process.

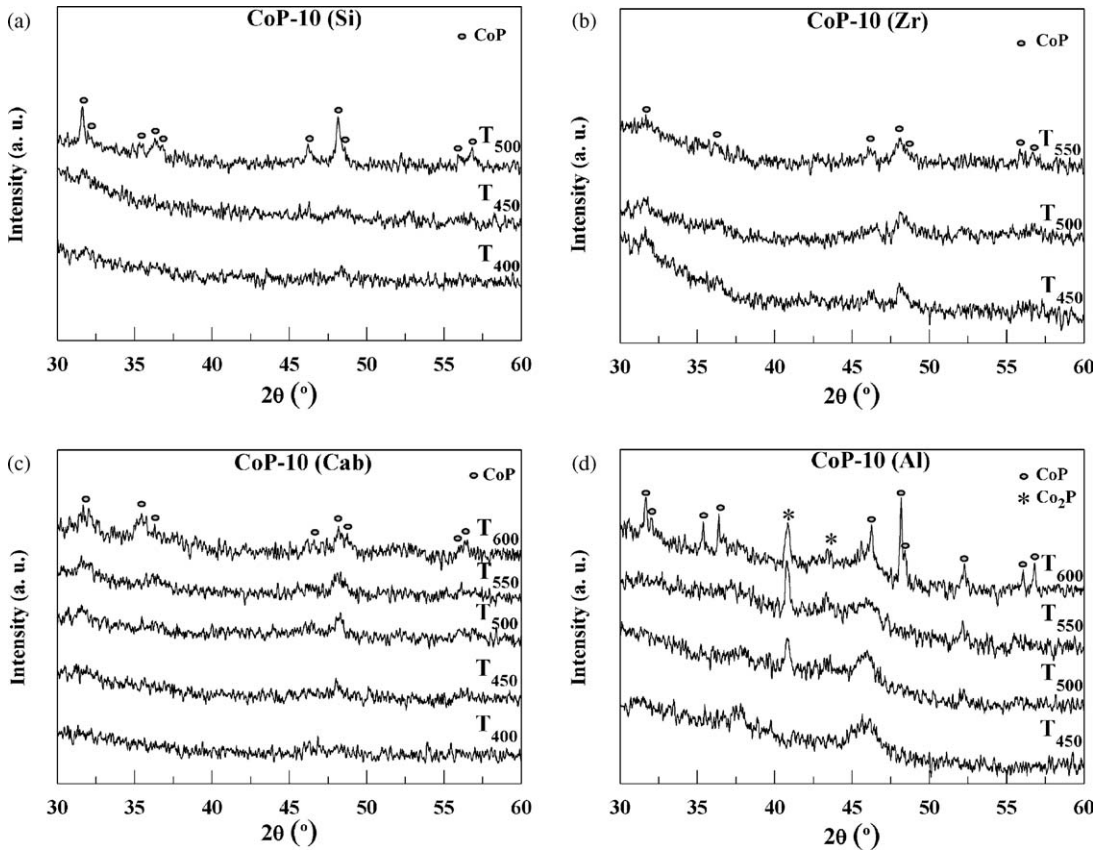

Fig. 3. X-ray diffractograms of: (a) CoP-10 (Si), (b) CoP-10 (Zr), (c) CoP-10 (Cab) and (d) CoP-10 (Al) catalysts, reduced at different temperatures. H_2 flow: 100 ml min^{-1}, heating rate: 3 °C min^{-1}.

3.1.3. CO chemisorption measurements

CO chemisorption measurements were carried out on both reduced and spent catalysts. These measurements provide the number of active cobalt sites (n_{CO}), as compiled in Table 1. The chemisorption values are very low and always much lower than those found in other phosphides, as in the case of Ni_2P [34]. Reduced catalysts prepared on mesoporous carriers, CoP-10 (Si) and CoP-10 (Zr), chemisorb more CO than those prepared from commercial materials. Wang et al. [34] attributed the relatively low CO chemisorption capacity of a CoP/SiO_2 catalyst to an excess of surface P or possibly O (not removed during the reduction) blocking adsorption sites. According to Burns et al. the decrease in CO chemisorption could be due to the incorporation of phosphorus. These authors found the values of chemisorption to follow the order: Co > Co_2P > CoP [17], mainly due to an inhibition of the formation of bridge-bonded CO species. The phosphorous excess or possibly oxygen (from the unreduced precursor) blocks the active sites, thus provoking a lower CO uptake [34] and hindering the chemisorption of CO on the CoP sites. On the other hand, we observe an increase in the CO uptake for CoP-10 (Al) and CoP-10 (Cab) spent catalysts. This indicates, as will be seen later, the presence of a greater amount of CoP formed during the HDS process, except in the case of CoP-10 (Zr) sample, where a decrease is observed.

Moreover, by assuming that the samples were composed of uniform spherical particles, the theoretical metal site concentrations (n_{sites}) were calculated [12] from the equation:

$$\text{Metal site concentration} = S_g n f,$$

where S_g is the specific surface area of cobalt phosphide (CoP); n is the average surface metal atom density (9.99×10^{14} atoms cm^{-2}); and f accounts for the fractional weight loading (g_{CoP}/g_{cat}). S_g is calculated by $S_g = 6/\rho D_c$, with ρ representing the density of cobalt phosphide (6.2 g cm^{-1}) and D_c being the crystallite size calculated by the Scherrer equation from the full width at half maximum (FWHM) of the XRD line located at $2\theta = 48.1°$ in CoP-10 (Si), CoP-10

Table 1
Metallic properties of reduced and spent catalysts.

Catalyst	d_{XRD} (nm)[a]			n_{sites} (μmol g^{-1})[b]			n_{CO} (μmol g^{-1})[c]		
	Initial	Spent (T)[d]	Spent (time)[e]	Initial	Spent (T)[d]	Spent (time)[e]	Initial	Spent (T)[d]	Spent (time)[e]
CoP-10 (Si)	62	58	72	39	42	34	5	2	4
CoP-10 (Zr)	30	42	55	82	58	44	5	1	1
CoP-10 (Cab)	32	41	31	76	60	79	1	6	5
CoP-10 (Al)	59	53	51	30	33	35	1	2	3

[a] Crystallite size calculated from XRD patterns using the Scherrer equation.
[b] Metal site concentration calculated from XRD particle size according to Ref. [12].
[c] Stoichiometry of CO/active site is assumed to be 1 for all the samples.
[d] Catalysts after the temperature test.
[e] Catalysts after the time test.

Table 2
Textural and acidic properties of the support and reduced catalysts.

Sample	S_{BET} ($m^2\,g^{-1}$)	V_p ($cm^3\,g^{-1}$)	d_p (av) (nm)	NH_3 ($\mu mol\,g^{-1}$)
MCM-41	644	0.394	2.4	174
CoP-10 (Si)	79	0.090	4.6	826
MCM-Zr	491	0.353	2.9	822
CoP-10 (Zr)	77	0.068	3.6	1113
Cab-osil	257	0.720	11.2	151
CoP-10 (Cab)	69	0.318	18.5	971
γ-Al_2O_3	268	0.346	5.2	323
CoP-10 (Al)	42	0.108	10.3	1325

(Zr) and CoP-10 (Cab) for CoP [34] and $2\theta = 40.8^\circ$ in CoP-10 (Al) for Co_2P. From this theoretical data, shown in Table 1, it can be seen that after the reduction process CoP-10 (Zr) and CoP-10 (Cab) provide a greater number of active sites.

The active site densities (n_{sites}) are totally different to those calculated from CO chemisorption; cobalt phosphide catalysts hardly chemisorb any CO. The n_{sites} value is calculated based on the assumption that all Co moles added are transformed into the corresponding phase, which is not entirely the case since all catalysts are partially reduced, particularly CoP-10 (Zr) and CoP-10 (Al) samples, which are reduced to a lesser extent. Anyhow, CoP-10 (Zr) and CoP-10 (Cab) possess the highest amount of n_{sites} for having the lowest particle size.

3.1.4. Textural properties

The textural properties of the supported cobalt phosphide catalysts are listed in Table 2. The results show a great loss of both surface area and pore volume with regard to the bare supports. We obtained similar results when preparing a Ni_2P phase following the same method. Although the decrease is more important for mesoporous based catalysts, the samples prepared with Cab-osil and γ-Al_2O_3 suffer a considerable decrease. Some authors suggest that the loss of surface area is due to the excess of phosphorous that causes the blockage of the pores [35]. In this sense, the corresponding N_2 isotherms for CoP-10 (Si) and CoP-10 (Zr) show the loss of part of the mesoporous nature, although the main characteristics of the IV type isotherm remain intact, which corroborates the likelihood that a partial blockage of the mesoporous structure does occur.

3.1.5. Acidic properties

The acidic properties of the catalysts were measured by thermoprogrammed desorption of ammonia (NH_3-TPD) between 100 and 550 °C. Table 2 compiles the total amount of NH_3 desorbed for supports and reduced catalysts. From the acidity data of the bare supports, we can see how MCM-Zr and γ-Al_2O_3 possess higher acidity values than pure silica based supports. These results agree well with the previous data discussed in the TPR experiments. These two supports were used for the catalysts (CoP-10 (Al) and CoP-10 (Zr)) that desorbed less water and phosphide during reduction. This reveals that the acidity of the support hinders the precursor from forming the active phase, due to a stronger precursor–support interaction. The same results have been found previously by the group of Bussell and co-workers [28]. On the other hand, comparing the ammonia desorbed, in all cases, the support desorbs less ammonia than reduced catalysts. This suggests that the presence of phosphorous or cobalt is responsible for the increased acidity of the catalysts compared to the bare support.

3.1.6. XPS

In order to investigate the surface composition of the precursor and reduced catalyst, XPS measurements were carried out. Table 3 shows the binding energy values for the precursor, the reduced and spent catalysts and the superficial atomic Co/P ratio for all of them.

Co $2p_{3/2}$ core level spectra (not shown) of all the precursor catalysts show two contributions. The first band is centred at *c.a.* 782.0 eV, and assigned to Co^{2+} ions forming $Co(HPO_3H)_2$, and the second band is a broad contribution due to the shake-up satellite assigned in the literature to a divalent species [36]. On the other hand, the P $2p_{3/2}$ core level spectra only show one signal with the maxima around 133.7 eV of phosphorous in the form of HPO_3H^- [37].

The Co/P theoretical bulk ratio is 0.5, however only the CoP-10 (Zr) and CoP-10 (Cab) precursors reflect this value at the surface. The other two precursors present cobalt enrichment on the surface.

Table 3
Spectral parameters obtained by XPS analysis.

Sample	Binding energy (eV)					Superficial	Atomic ratio
	Co $2p_{3/2}$		P $2p_{3/2}$				
	Co^{2+}	CoP	HPO_3^-	PO_4^-	CoP	Co/P	Co/X
Precursors							
CoP-10 (Si)	781.6	–	133.8	–	–	1.10	0.19
CoP-10 (Zr)	782.2	–	133.7	–	–	0.62	0.40
CoP-10 (Cab)	782.2	–	133.8	–	–	0.43	0.05
CoP-10 (Al)	782.1	–	133.6			0.93	0.85
Catalysts							
CoP-10 (Si)	782.0	778.1	133.2	134.4	128.8	0.54	0.26
CoP-10 (Zr)	782.6	778.6	133.6	134.5	129.1	0.43	0.45
CoP-10 (Cab)	782.2	778.6	133.2	134.5	128.9	0.30	0.03
CoP-10 (Al)	782.2	777.7	133.9	134.8	128.9	0.21	0.53
Spent catalysts (after temperature reduction)							
CoP-10 (Si)	781.9	778.6	133.4	134.4	129.7	0.73	0.18
CoP-10 (Zr)	781.5	778.2	133.3	134.4	128.9	0.43	0.56
CoP-10 (Cab)	782.1	778.5	133.0	134.2	129.0	0.50	0.04
CoP-10 (Al)	782.1	778.1	133.6	134.7	129.0	0.52	0.50
Spent catalysts (after time reduction)							
CoP-10 (Si)	781.0	778.2	133.0	134.6	129.3	1.00	0.67
CoP-10 (Zr)	781.4	778.3	133.3	134.4	129.1	0.54	0.53
CoP-10 (Cab)	782.1	778.5	133.2	134.6	129.0	0.49	0.05
CoP-10 (Al)	782.1	778.0	133.6	134.7	129.0	0.59	0.43

X = (Si for CoP-10 (Si) and CoP-10 (Cab), (Si + Zr) for CoP-10 (Zr) and Al for CoP-10 (Al)).

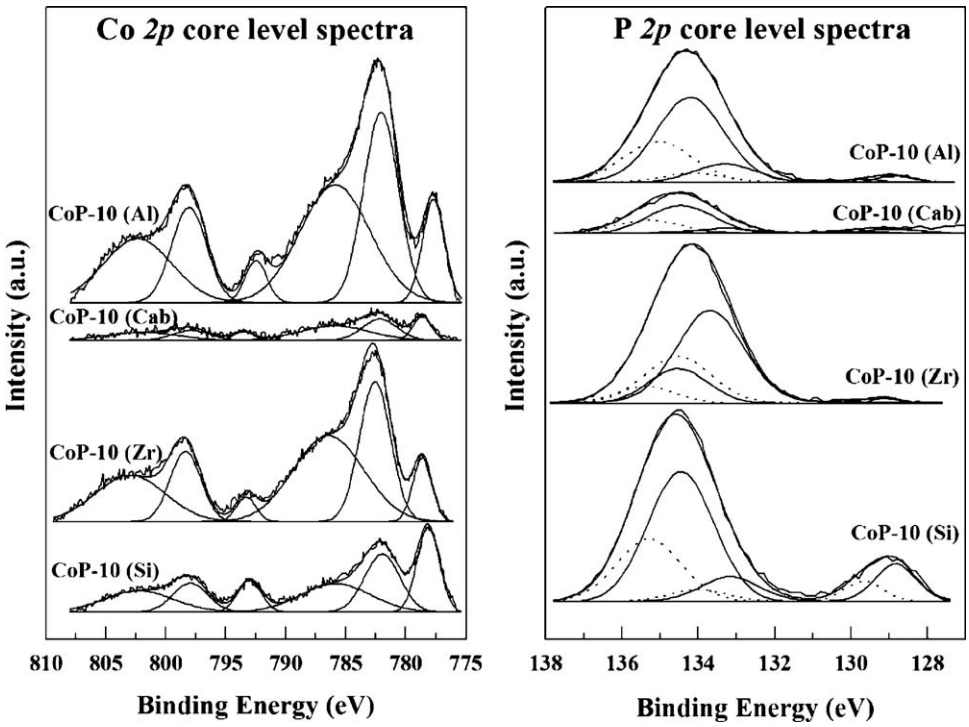

Fig. 4. XPS spectra for CoP-10 catalysts over different supports.

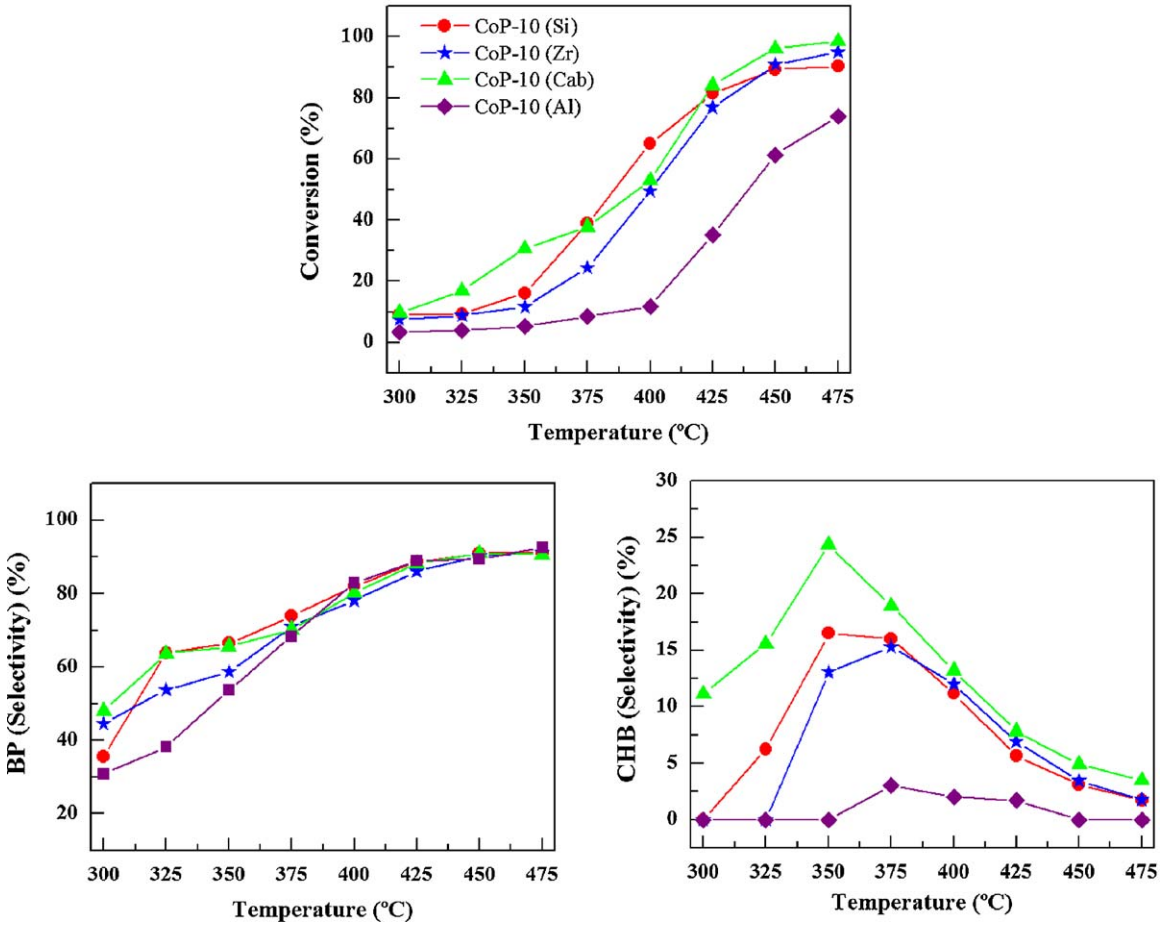

Fig. 5. Evolution of conversion and selectivity as a function of temperature for CoP-10 catalysts over different supports.

Table 4
Conversions, selectivities and turn over rates for dibenzothiophene HDS.

Catalyst	Conversion (%)		Selectivity (%)				TOF × 10^3 (s^{-1}) from n_{sites}[a]		
	T[b]	Time[c]	T[b]		Time[c]		Initial	Spent (T)[b]	Spent (time)[c]
			BP	CHB	BP	CHB			
CoP-10 (Si)	90.3	67.0	91.3	1.7	86.7	9.9	0.19	3.0	4.1
CoP-10 (Zr)	95.0	60.0	91.1	1.8	89.2	4.6	0.56	2.5	2.8
CoP-10 (Cab)	98.6	98.4	90.8	3.5	90.3	8.0	0.56	2.4	1.8
CoP-10 (Al)	74.0	30.2	92.5	0	86.8	1.8	1.77	4.4	2.0

[a] Calculated from data compiled in Table 1.
[b] Catalysts after the temperature test at 475 °C.
[c] Catalysts after 48 h of reaction.

In the case of reduced catalysts, the Co 2p core level spectra for all samples are depicted in Fig. 4. From this plot, we observe that the Co $2p_{3/2}$ signal possesses a new contribution located at *c.a.* 778.5 eV [38]. This contribution appears as a consequence of the formation of CoP and/or Co_2P. Binding energy values of 778.1 eV for CoP and 778.3 eV for Co_2P have been published in the literature [38]. The peak at 778.1 eV for CoP-10 (Si) and at 778.6 eV for both CoP-10 (Zr) and CoP-10 (Cab) should be due to the presence of CoP, while the band at 777.7 eV for CoP-10 (Al) comes from the formation of Co_2P, according to XRD results. Nonetheless, we cannot discard the presence of small CoP particles that could go undetected by the XRD technique and that can also contribute to this peak. The surprising fact is that CoP-10 (Zr) and especially CoP-10 (Al), exhibit the Co 2p signals more intensely, which suggests a greater presence of Co on the surface of these samples, it should be taken into account that these two samples favour the formation of Co_2P (Fig. 2), that is a cobalt rich phase, and is responsible of the higher presence of cobalt on the surface of these two samples. Thus, the highest Co/X ratios (X = Si, Si + Zr or Al, accordingly) were found for CoP-10 (Al) and CoP-10 (Zr) reduced catalysts, with a value of 0.53 and 0.45, respectively (Table 3). Meanwhile, CoP-10 (Cab) possesses the lowest ratio (0.03) according to the noisy Co 2p signal observed.

The P 2p signals of reduced catalysts are showed in Fig. 4. A new contribution is observed at binding energy values of 129.2 eV, and assigned to reduced phosphorous in the form of cobalt phosphide, $P^{\delta-}$ in CoP or Co_2P, accordingly [38]. The peak at 133.3 eV is due to unreduced (HPO_3H^-) species that indicates a partial reduction of the precursor [31] and finally, the band at 134.5 eV is typical of a phosphate species [17] and appears after a superficial oxidation of phosphide to phosphate due to air contact, which increases when the formation of phosphide is higher. Hence, although air

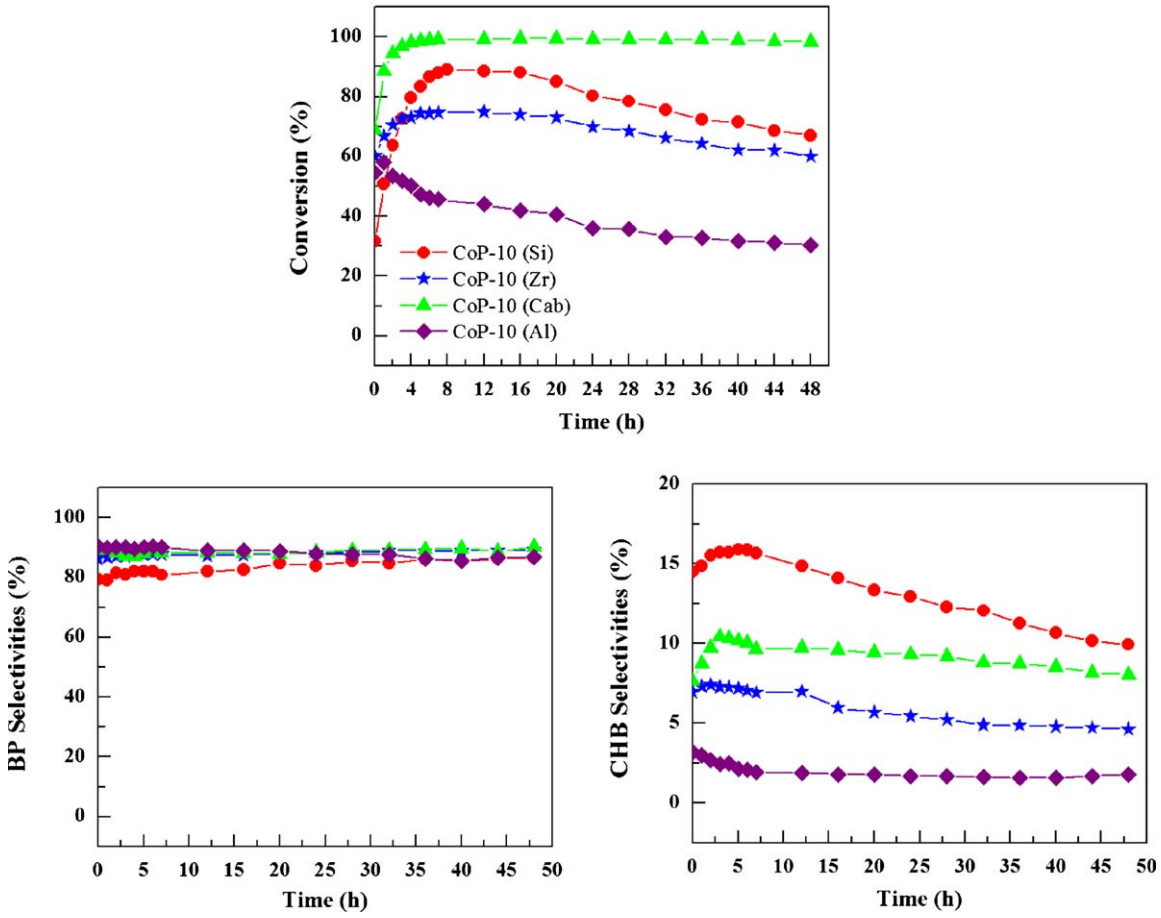

Fig. 6. Evolution of conversion and selectivity as a function of time on stream for CoP-10 catalysts over different supports.

exposure is avoided during the XPS, a partial oxidation can take place.

After the reduction process, the Co/P ratio decreases in all cases, which suggests a superficial phosphorous enrichment taking place during the reduction process, and can also be partially related to a passivation layer [39], as stated before. This superficial phosphorous enrichment, as previously suggested, confirms the low CO chemisorption capacity of these catalysts. Burns et al. [17] have obtained with a Co_xP_y/SiO_2 catalyst having an initial P/Co molar ratio of 2 in the oxidic precursor, a value similar to that of our catalysts, a superficial Co/P ratio of 0.87 after the reduction. This value is higher than that of ours, which reflects a higher surface phosphorous enrichment of our systems. It should be considered here that during the reduction process some phosphorous is lost as PH_3, this loss being more important at higher temperatures. These authors perform the reduction until 650 °C, meanwhile we only achieve 500 °C and as a consequence the surface of our catalysts exhibits a phosphorous enrichment. Although there is no data reported for CoP catalysts, some authors [28] have pointed out for Ni_2P based catalysts that during the test some phosphorous is lost; therefore the excess of phosphorous could have the function of keeping the supported Ni_2P particles fully phosphided during the catalytic test. The same should be happening in CoP catalytic systems.

3.2. Catalytic results

The catalysts prepared have been tested in the HDS of dibenzothiophene. HDS activity was first studied by varying the reaction temperature. Fig. 5 plots the corresponding results and Table 4 compiles the conversion and selectivity values obtained. At low reaction temperatures all supports have similar conversions, of about 5–10%, however when the temperature increases, all the catalysts, with the exception of CoP-10 (Al), reach high conversion values, ranging between 85% and 95%.

With regard to selectivity (Fig. 5), two main products were detected; BP, coming from the direct desulfurization (DDS) pathway, which is the preferential one in all catalysts, and CHB, coming from the hydrogenation (HYD) pathway [31] and formed to a lesser extent. It has been fully described in the literature that phosphide catalysts favour the HDS of dibenzothiophene through the DDS route. On the other hand, and as expected, the selectivity towards BP increases with temperature in a similar way to the conversion, reaching values close to 90% in all cases. Moreover, it should be noted that at low temperatures (325 and 350 °C) silica based catalysts, CoP-10 (Cab) and CoP-10 (Si), favour its formation. With regard to CHB selectivity, it is favoured at intermediate temperatures. Silica based catalysts favour its formation up to 350 °C, while at $T \geq 375$ °C, CoP-10 (Si), CoP-10 (Zr) and CoP-10 (Cab) show a similar pattern. Hydrogenation reaction is not favoured at high temperatures because of thermodynamic considerations, that is why the formation of CHB decreases while increasing the temperature. It is always the CoP-10 (Cab) catalyst which shows the best selectivity patterns to this compound and it is related to its smaller particle size. The DBT interaction with small particles, through the S-atom, generates a strong bond to the cobalt centres and moreover, due the small particle size, the molecules can swing around provoking the interaction of the phenyl ring with the surface, where it can be hydrogenated [40].

CoP-10 (Al) showed the lowest selectivity to CHB. The CoP-10 (Al) catalyst possesses Co_2P as an active phase according to XRD results. Therefore we can conclude that this phase is less active

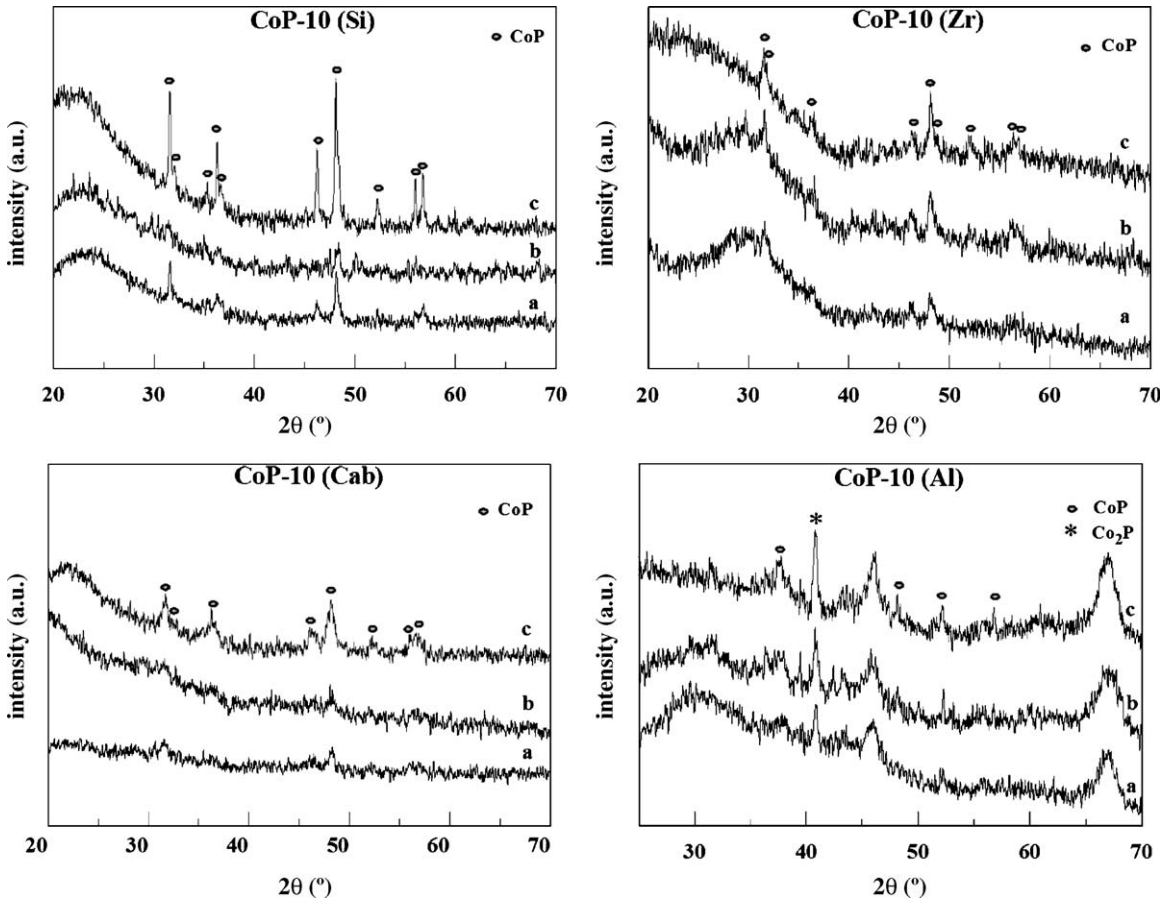

Fig. 7. X-ray diffractograms of fresh and spent catalysts over different supports.

than CoP itself, as previously reported in the literature [17] and is also less selective to the hydrogenation products, only performing the DBT HDS reaction through the DDS route.

Following these results, and in order to study the stability of these catalysts, they were tested for 48 h at 400 °C in the case of CoP-10 (Si), CoP-10 (Zr) and CoP-10 (Cab), and 450 °C in the case of CoP-10 (Al). The corresponding results are compiled in Fig. 6 and Table 4. In general, they all show increased activity during the first hours on stream, although CoP-10 (Al) undergoes a gradual deactivation after the third hour. The catalysts prepared with mesoporous materials, CoP-10 (Si) and CoP-10 (Zr), show an activity of 84% and 74%, respectively after 16 h on stream. After this, their activity gradually decreases, with conversion values of 67% and 60% obtained after 48 h on stream. Contrary to this is CoP-10 (Cab) catalyst, which shows an increase in its activity in the first few hours, reaching a conversion close to 100% after 4 h. Moreover, this catalyst does not suffer deactivation after 48 h on stream, displaying high stability. As regards the selectivity, the main product of all the catalysts is BP, resulting from the DDS pathway. The selectivity to this product is constant throughout the reaction time. Except this CoP-10 (Cab) catalyst, the product of the HYD pathway, such as CHB, suffers deactivation after the first few hours of the reaction. So, when the conversion decreases, the only impaired route is that of the HYD pathway. In the case of CoP-10 (Al), CHB production is not noticeable during the time on stream.

3.3. Evolution of the active phase during the catalytic test

A novel synthetic approach to preparing a series of supported CoP catalysts has proved to be very effective in DBT HDS. Catalyst characterization by XRD and XPS analysis confirmed the presence of cobalt phosphide on the supported catalysts.

The synthesis of silica supported cobalt phosphide catalysts by the TPR method has been described in the literature, although in all cases cobalt phosphate based precursors have been used to form the corresponding cobalt phosphide phase, with the Co/P molar ratio determining the formation of either CoP or Co_2P. Moreover, high hydrogen flows have been employed. Wang et al. used a H_2 flow rate of 1500 ml min^{-1} [34] while Burns et al. [17] employed 300 ml min^{-1}. The activity data for cobalt phosphide catalysts reported in the literature has been lower than those for nickel phosphide catalysts in HDS reactions [17,34]. In this work the preparation of cobalt phosphide catalysts by a novel and easy synthetic approach is described: a phosphorous precursor salt with a lower phosphorous oxidation state, and therefore easier to reduce, is used. The step of calcination is precluded, and a relatively low hydrogen flow of only 100 ml min^{-1} is required. Furthermore, the study of the catalytic activity in DBT HDS provides excellent results. Hence, the influence of the reaction temperature provided catalytic conversions close to 100% at 475 °C, except in the case of the CoP-10 (Al) catalyst, which presented the lowest activity at all

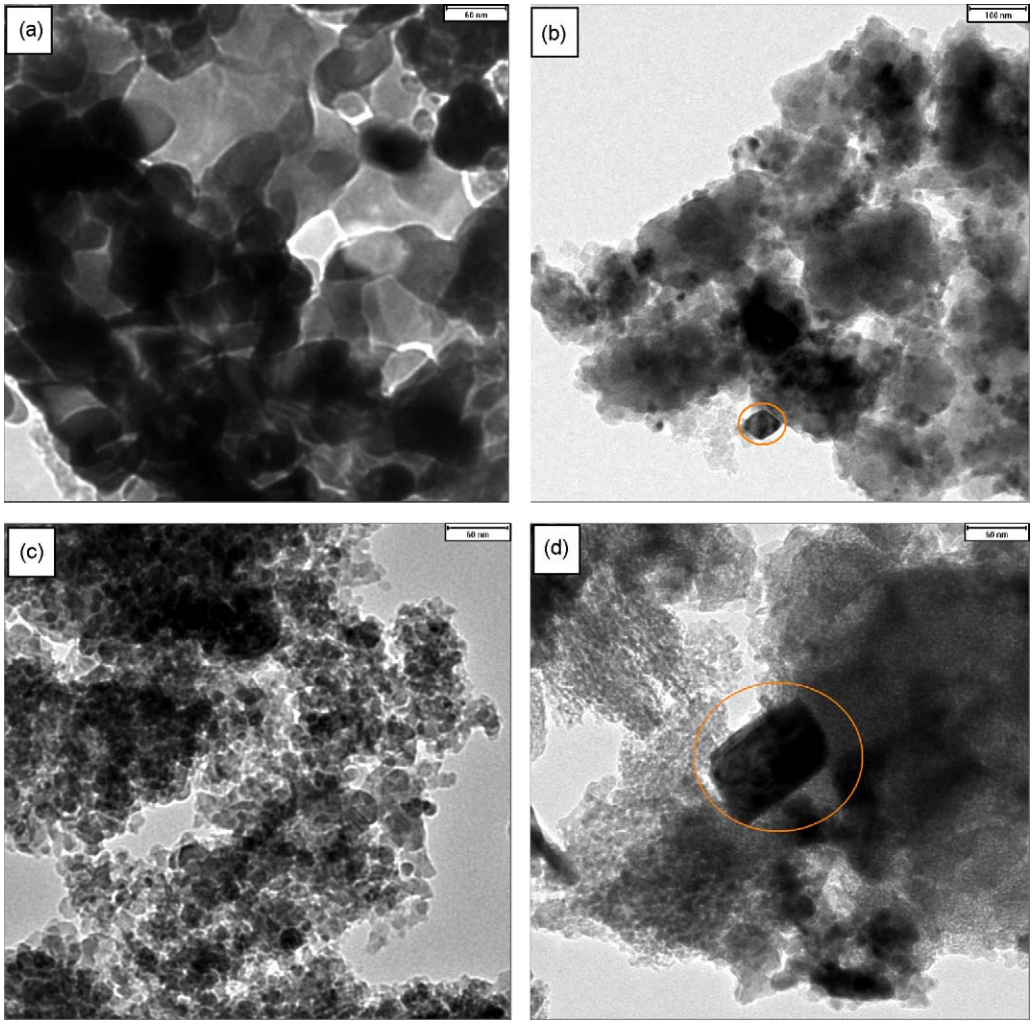

Fig. 8. TEM micrographs of spent catalysts (after time test): (a) CoP-10 (Si) (60 nm scale), (b) CoP-10 (Zr) (100 nm scale), (c) CoP-10 (Cab) (60 nm scale) and (d) CoP-10 (Al) (60 nm scale).

the temperatures studied. The study of the catalytic stability for 48 h revealed that the commercial silica Cab-osil is the most appropriate support for preparing highly active cobalt phosphide catalysts, still maintaining high activity after 48 h on stream. Contrary to expected, mesoporous based catalysts, CoP-10 (Si) and CoP-10 (Zr), underwent a gradual deactivation with time on stream. CoP-10 (Al) catalysts suffered a deep deactivation after the third hour of reaction. The activity found with CoP-10 (Cab) catalyst is much higher than the data published so far in the literature where a CoP catalyst supported on silica possessed a conversion of dibenzothiophene close to 50% after 48 h working [34]. Furthermore, the activity is similar to that found for a Ni_2P catalysts [31,41] tested under the same experimental conditions, i.e., similar conversion and selectivity values are attained. In this sense, a Ni_2P catalyst supported on silica Cab-osil, presented a conversion value close to 100% after 48 h on stream [41].

In order to understand the performance of these catalysts, XRD, XPS, CO chemisorption and TEM analyses were carried out on the catalysts after these reactions. In general, the catalysts after both reactions will be referred to as spent catalysts.

XRD measurements for spent samples after both temperature and time testing, are compiled in Fig. 7. The catalyst structure for CoP-10 (Si), CoP-10 (Zr) and CoP-10 (Cab) samples was completely stable under the reaction conditions. The XRD analysis demonstrates that all the lines belonging to CoP remain intact, with these diffraction lines corresponding exclusively to this compound. Moreover it can be observed an increase in the intensity of the XRD peaks, mainly after the time test, which could indicate both the formation of a more active phase in the hydrotreating process and/or the formation of a greater number of diffraction domains, i.e., an increment in the particle size. The measurement of the particle sizes in these samples (Table 1) was carried out by applying the Scherrer equation. It confirms growth of the active phase, although for CoP-10 (Cab) the change in the particle size is minimal. Similarly, CoP-10 (Al) catalyst shows the diffraction lines of the Co_2P phase in all cases, which becomes more intense after reaction. By calculating the Co_2P particle size for this spent catalyst (Table 1), it can be seen that the particle size hardly suffers any modification, besides it slightly diminishes after the temperature and time test. This suggests that the formation of more Co_2P phase does not take place during the catalytic reaction. Moreover, tiny diffraction lines arising from the presence of CoP also arise during the test. As stated before, the CoP phase could be formed due to the reaction of PH_3 with Co_2P. CoP-10 (Al) catalyst possesses an excess of phosphorous remaining on the surface, according to the H_2-TPR experiments, due to a strong phosphorous–alumina interaction. It has been reported that PH_3 could be formed during the catalytic test [34], which could in turn react with Co_2P particles to form a CoP phase. This would mean that at elevated temperatures and under the reducing conditions imposed during the catalytic test, the P containing surface is reduced, and incorporated into the catalyst [42].

The micrographs for spent catalysts obtained by TEM (Fig. 8) confirm the differences between the catalysts, depending on the support employed. Moreover, EDAX analysis let us know the bulk composition of the particles analyzed. CoP-10 (Si) (micrograph a) shows defined particles with sizes between 60 and 70 nm, which is consistent with those obtained from XRD. Moreover, an EDAX

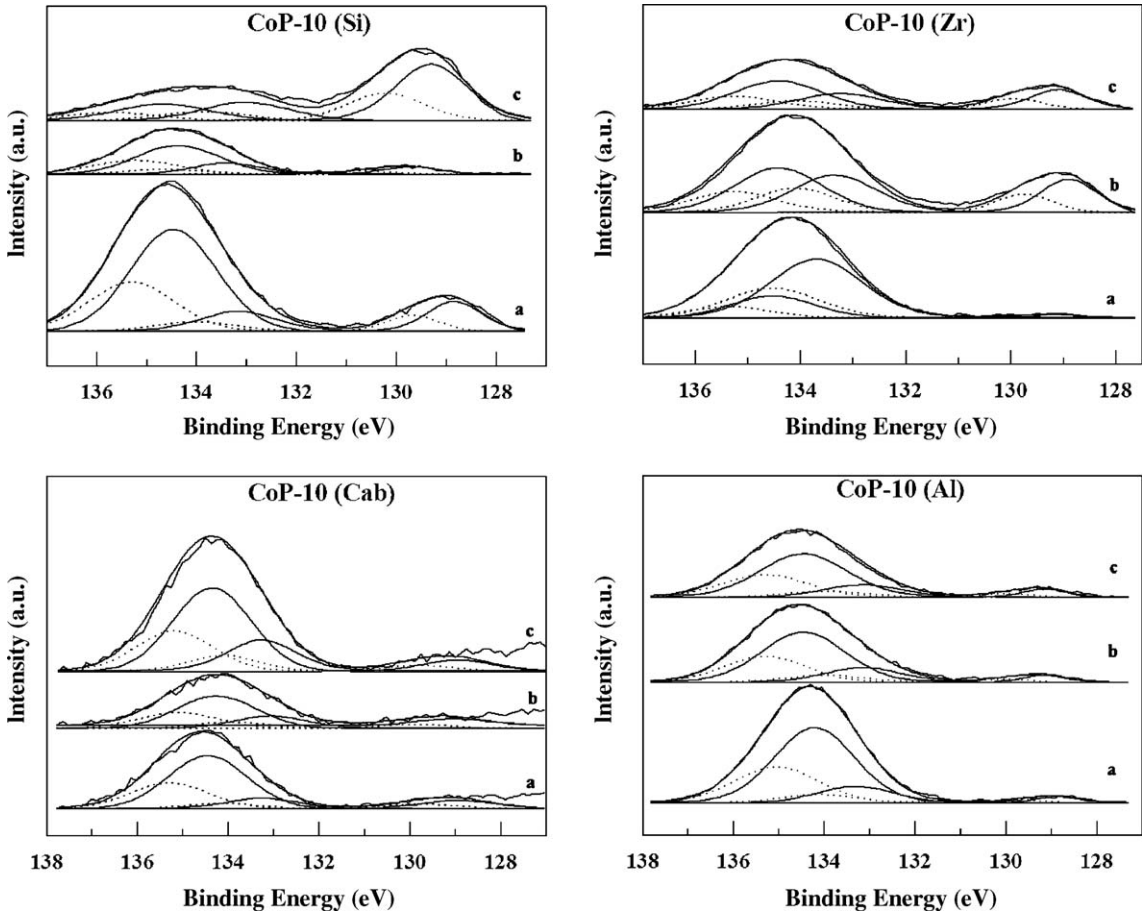

Fig. 9. P 2p core level spectra of fresh and spent catalysts over different supports: (a) reduced catalyst, (b) spent catalyst after temperature test and (c) spent catalyst after time test.

analysis of these particles provided an atomic Co/P ratio of 0.98, which confirms the formation of the CoP phase. CoP-10 (Zr) catalyst shows a different pattern, where particles appear in different sizes (micrograph b). The presence of unreduced species on this sample has been described previously, and corresponds to small dispersed particles. EDAX analysis of this zone provided an atomic Co/P ratio of 0.4. The EDAX analysis on the particle indicated, with a size of *c.a.* 50 nm (as found by XRD analysis), reported an atomic Co/P ratio of 0.87, close to the theoretical ratio of 1. The CoP-10 (Cab) catalyst (micrograph c) reveals the globular nature of the cobalt phosphide phase, with highly dispersed small particles being found, as by other authors [17], with particle sizes of the same order of magnitude as those found by XRD; around 30 nm. EDAX analysis of this zone gave an atomic Co/P ratio of 0.97, which reveals that these dispersed particles also correspond to the CoP phase. Finally CoP-10 (Al) catalyst (micrograph d), possesses particles with sizes between 60 and 70 nm (a little higher than the values obtained by XRD) that provided an atomic Co/P ratio of 2.25, according to the EDAX analysis. This data also corroborates the formation of the Co_2P phase on this support.

XPS analyses for spent catalysts are shown in Figs. 9 and 10 and their binding energies are summarized in Table 2. P 2p signals were analyzed after temperature and time tests, respectively (Fig. 9). In all cases, the same contributions that were cited in the reduced catalysts were observed. The signal assigned to $P^{\delta-}$, corresponding to cobalt phosphide and centred at *c.a.* 129.0 eV, increases in the spent catalysts. This is reflected by XRD measurements, and indicates the formation of more active phase [12]. On the other hand, the intensity of the $P^{\delta-}$ band correlates with the intensity of the PO_4^{3-} signal (Table 2), due to a partial oxidation of the cobalt phosphide [18].

Fig. 10 shows the Co 2p signals for the spent catalysts. The peak centred at *c.a.* 778.5 eV, and assigned to cobalt phosphide, undergoes a considerable increase in the case of CoP-10 (Si) and CoP-10 (Zr) spent samples, as occurred for the P 2p signal. The reaction conditions seem to favour the formation of more active phase from unreduced species. On the other hand, CoP-10 (Cab) sample, which has the smallest particle size, shows the band intensity unmodified under the catalytic conditions. The Co 2p signal is also less intense than that for the other catalysts due to the presence of small and well dispersed particles, as is also detected by TEM micrographs. CoP-10 (Al) catalyst does not suffer any apparent modification of the Co 2p signal, except for a slight shift and an increase in the intensity of the $Co^{\delta+}$ signal at 777.7 eV at a higher BE. The formation of CoP, as detected by XRD, is responsible for both changes.

With regard to the superficial atomic Co/P ratios (Table 3) obtained by XPS, they increase with respect to reduced catalysts, after both time and temperature tests. Several aspects must be considered here. In general, the formation of a more active phase takes place during the reaction. Further, the possible loss of phosphorous during the reaction could also be responsible for this ratio increase. With the exception of CoP-10 (Si), the spent catalysts have a similar ratio close to 0.5.

The analysis of the S 2p signal for spent catalysts revealed the presence of sulfur in some samples. It has been reported that the introduction of small amounts of sulfur improves the catalytic properties of nickel phosphide catalysts in HDS reactions due to

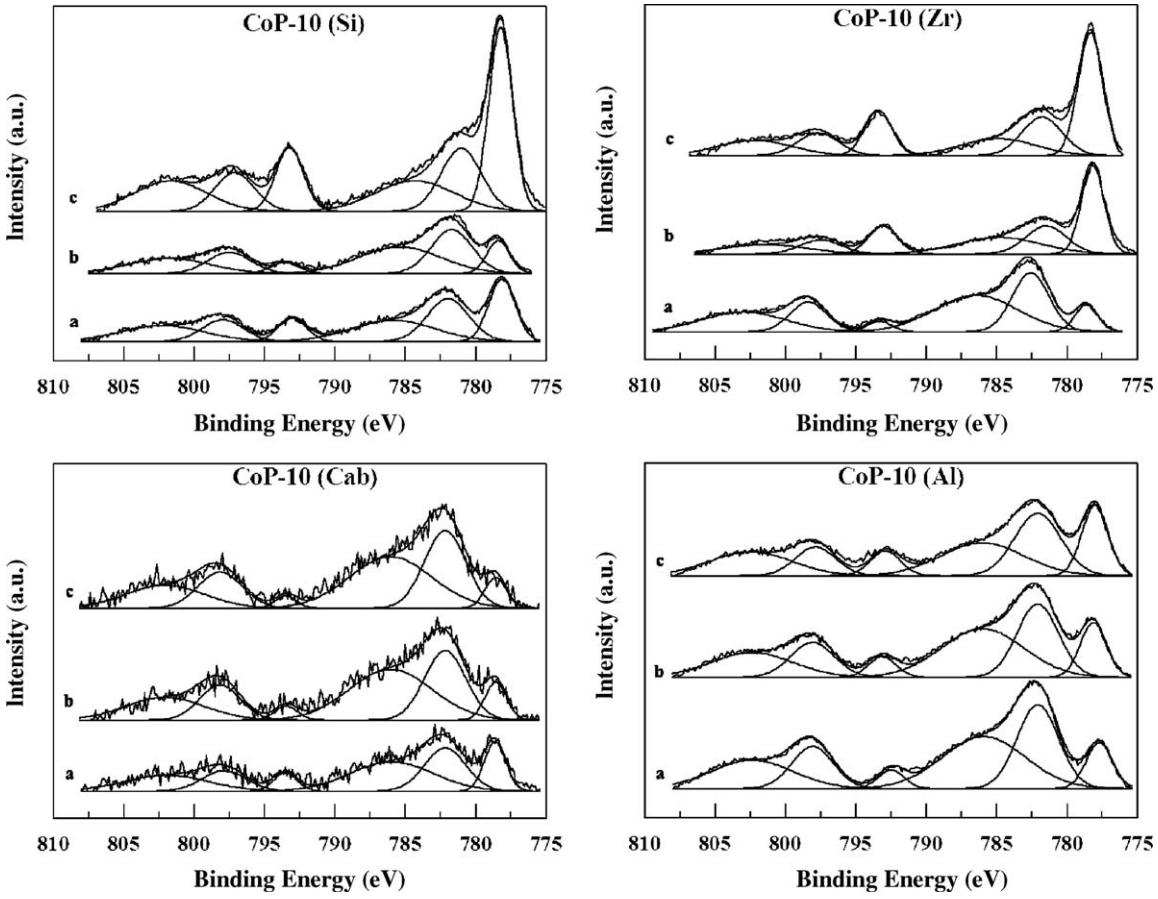

Fig. 10. Co 2p core level spectra of fresh and spent catalysts over different supports: (a) reduced catalyst, (b) spent catalyst after temperature test and (c) spent catalyst after time test.

the formation of a NiP_xS_y phase [18,22,28]. The literature devoted to the study of phosphosulfide species in cobalt phosphide catalysts is scarce, although the formation of CoP_xS_y has been reported [17] on cobalt phosphide catalysts. Also, depending on the kind of cobalt phosphide phase present on the surface, the incorporation of sulfur to obtain a phosphosulfide phase changes. Thus, the Co_2P species captures more sulfur on the surface than the CoP phase [17]. The acidity of the support is a key factor in obtaining a phosphosulfide. Catalysts with higher acidity such as CoP-10 (Zr) and CoP-10 (Al) have 0.49% and 0.73% of superficial atomic sulfur (obtained by XPS analysis), respectively after the temperature test, which corroborates that the Co_2P phase retains more sulfur than the CoP phase. Silica based catalysts, CoP-10 (Si) and CoP-10 (Cab), display a weaker CoP–support interaction, meaning sulfur incorporated onto the CoP surface is more easily hydrogenated, thus regenerating the Co sites. On the most acidic supports, CoP-10 (Zr) and CoP-10 (Al), the S incorporated into the cobalt phosphide phase is not as susceptible to hydrogenation and removal as H_2S and therefore the superficial phosphosulfide formed could be less active. With the exception of CoP-10 (Al), all catalysts reach the same level of activity (Fig. 5), which confirms the literature data: Co_2P is less active than CoP. After time testing, CoP-10 (Si) has sulfur on its surface (1%), which can be explained by the large amount of active phase present on this sample. Meanwhile, the CoP-10 (Al) catalysts also present 0.49% of surface sulfur.

The catalytic activity with time on stream reveals that the more active catalysts are those with lower acidity [40] (CoP-10 (Si) and CoP-10 (Cab)), probably due to the greater amount of active phase formed after the reduction. However, CoP-10 (Si) suffers deactivation due to the agglomeration of the active phase. CoP-10 (Zr) also deactivates, and an agglomeration of the active phase is also observed. A surprising result however is that no sulfur was detected on this sample by XPS, although a partial passivation could have happened, thus hindering its detection. The lower activity of the Co_2P phase is clearly demonstrated by the performance of the CoP-10 (Al) catalyst, which moreover suffers a considerable deactivation after 48 h on stream. It has been reported that the P-rich metal phosphide phase (i.e., CoP) is more active than the more metal-rich phosphide phase (i.e., Co_2P) [28,43], with the introduction of phosphorous leading to deactivation resistant catalysts.

The CO chemisorption capacities of the spent catalysts (Table 1) are very low, with the CoP-10 (Cab) catalyst being that which possesses the highest values. This is related to its higher dispersion. The data complied in Table 4 shows the turnover frequency (TOF), calculated from theoretical n_{sites}. Initially they all possess low TOF values, while after temperature testing, they all reach TOF values similar to those obtained for the Ni_2P based catalysts [31,34], but higher than those reported for cobalt phosphide catalysts [34] prepared by the traditional method. TOF values after time testing are also compiled in Table 4. Surprisingly, it is the CoP-10 (Cab) catalyst that presents the highest stability and conversion values, giving a lower TOF value than the CoP-10 (Si) and CoP-10 (Zr) samples. These results suggest that the larger particles on the CoP-10 (Zr) and CoP-10 (Si) catalysts are as active as the smaller particles on the CoP-10 (Cab) catalyst. However, the small CoP particles on the CoP-(Cab) catalyst are more stable, since high conversion values are maintained, and they do not agglomerate.

It has been reported that the TOF values, as well as the CO chemisorption in CoP, are lower than those for Ni_2P [17], since nickel phosphide is more resistant to sulfur incorporation than cobalt phosphide catalysts. Consequently, Ni_2P is a more active catalyst in the HDS reaction. However, CoP-10 (Cab) catalyst exposed here displays high conversion values and stability similar to that found with Ni_2P catalysts [31,41].

4. Conclusions

The synthesis of differently supported cobalt phosphide catalysts by the novel and easy synthetic approach exposed here provides a highly active catalyst when silica Cab-osil was employed as material support, CoP-10 (Cab). The support employed determines the cobalt phosphide phase formed, i.e., when MCM-Si, MCM-Zr and silica Cab-osil are used only CoP phase is formed, in contrast, with γ-Al_2O_3, the Co_2P phase is the main phase detected. On the other hand, the catalytic activity of these catalysts in DBT HDS provides excellent results. The influence of the reaction temperature shows that catalytic conversions close to 100% are attained at 475 °C, except in the case of the catalyst prepared on γ-Al_2O_3 as support (CoP-10 (Al)), which presented the lowest activity at all the temperatures studied due to the formation of a less active cobalt phosphide phase, Co_2P, on this support. The study of the catalytic stability for 48 h revealed that the commercial silica Cab-osil is the most appropriate support for preparing highly active cobalt phosphide catalysts, still maintaining high activity after 48 h on stream. Contrary to expected, mesoporous based catalysts, CoP-10 (Si) and CoP-10 (Zr), underwent a gradual deactivation due to the agglomeration of the active phase; meanwhile CoP-10 (Al) suffered a rapid deactivation after the third hour of reaction as a consequence of the presence of the less active Co_2P phase.

Acknowledgements

We gratefully acknowledge the support from the Ministry of Education and Science, Spain (Ministerio de Educación y Ciencia, España) through the projects MAT2006-02465 and MAT2009-10481 and from the Regional Andalusian Government (Junta de Andalucía) through the Excellence Project P06-FQM-01661. J.A.C.B. thanks the Ministry of Education and Science, Spain (Ministerio de Educación y Ciencia, España) for a fellowship (BES-2007-15735). A.I.M. thanks the Regional Andalusian Government (Junta de Andalucía) for a postdoctoral contract.

References

[1] T.C. Ho, Catal. Today 98 (2004) 3–18.
[2] J.J. Lee, H. Kim, S.H. Monn, Appl. Catal. B 41 (2003) 171–180.
[3] H. Topsøe, B.S. Clausen, F.E. Massoth, in: J.R. Anderson, M. Boudart (Eds.), Catalysis-Science and Technology, vol. 11, Springer-Verlag, Berlin, 1991.
[4] R. Prins, V.H.J. de Beer, G.A. Somorjai, Catal. Rev. 31 (1989) 1–41.
[5] B. Pawelec, J.L.G. Fierro, A. Montesinos, T.A. Zepeda, Appl. Catal. B 80 (2008) 1–14.
[6] W.R.A.M. Robinson, J.N.M. van Gestel, T.I. Korányi, S. Eijsbouts, A.M. van der Kraan, J.A.R. van Veen, V.H.J. de Beer, J. Catal. 161 (1996) 539–550.
[7] P. Liu, J.A. Rodríguez, J.T. Muckerman, J. Mol. Catal. A 239 (2005) 116–124.
[8] B. Diaz, S.J. Sawhill, D.H. Bale, R. Main, D.C. Phillips, S. Korlann, R. Self, M.E. Bussell, Catal. Today 86 (2003) 191–209.
[9] M. Nagai, Appl. Catal. A 322 (2007) 178–190.
[10] G.L. Parks, M.L. Pease, A.W. Burns, K.A. Layman, M.E. Bussell, X. Wang, J. Hanson, J.A. Rodriguez, J. Catal. 246 (2007) 277–292.
[11] S.T. Oyama, X. Wang, Y.-K. Lee, W.-J. Chun, J. Catal. 221 (2004) 263–273.
[12] S.T. Oyama, X. Wang, Y.-K. Lee, K. Bando, F.G. Requejo, J. Catal. 210 (2002) 207–217.
[13] E. Furimsky, Appl. Catal. A 240 (2003) 1–28.
[14] F. Nozaki, M. Takumi, J. Catal. 79 (1983) 207–210.
[15] W. Li, B. Dhandapani, S.T. Oyama, Chem. Lett. 3 (1998) 207–208.
[16] S.J. Sawhill, D.C. Phillips, M.E. Bussell, J. Catal. 215 (2003) 208–219.
[17] A.W. Burns, K.A. Layman, D.H. Bale, M.E. Bussell, Appl. Catal. A 343 (2008) 68–76.
[18] S.T. Oyama, J. Catal. 216 (2003) 343–352.
[19] V. Zuzaniuk, R. Prins, J. Catal. 219 (2003) 85–96.
[20] S. Yang, C. Liang, R. Prins, Stud. Surf. Sci. Catal. 162 (2006) 307–314.
[21] C. Stinner, R. Prins, T. Weber, J. Catal. 202 (2001) 187–194.
[22] F. Sun, W. Wu, Z. Wu, J. Guo, Z. Wei, Y. Yang, Z. Jiang, F. Tian, C. Li, J. Catal. 228 (2004) 298–310.
[23] A.W. Burns, A.F. Gaudette, M.E. Bussell, J. Catal. 260 (2008) 262–269.
[24] S.T. Oyama, T. Gott, H. Zhao, Y.-K. Lee, Catal. Today 143 (2009) 94–107.
[25] K.A. Layman, M.E. Bussell, J. Phys. Chem. B 108 (2004) 10930–10941.
[26] C. Stinner, Z. Tang, M. Haouas, T. Weber, R. Prins, J. Catal. 208 (2002) 456–466.
[27] D. Ferdous, N.N. Bakhshi, A.K. Dalai, J. Adjaye, Appl. Catal. B 72 (2007) 118–128.

[28] S.J. Sawhill, K.A. Layman, D.R. van Dik, M.E. Engelhard, C. Wang, M.E. Bussell, J. Catal. 231 (2005) 300–313.
[29] A. Wang, L. Ruan, Y. Teng, X. Li, M. Lu, J. Ren, Y. Wang, Y. Hu, J. Catal. 229 (2005) 314–321.
[30] T.I. Korányi, Z. Vít, D.G. Poduval, R. Ryoo, H.S. Kim, E.J.M. Hensen, J. Catal. 253 (2008) 119–131.
[31] J.A. Cecilia, A. Infantes-Molina, E. Rodríguez-Castellón, A. Jiménez-López, J. Catal. 263 (2009) 4–15.
[32] U. Ciesla, F. Schüth, Microporous Mesoporous Mater. 27 (1999) 131–149.
[33] E. Rodríguez-Castellón, A. Jiménez-López, P. Maireles-Torres, D.J. Jones, J. Rozière, M. Trombetta, G. Busca, M. Lenarda, L. Storaro, J. Solid State Chem. 175 (2003) 159–169.
[34] X. Wang, P. Clark, S.T. Oyama, J. Catal. 208 (2002) 321–331.
[35] I.I. Abu, K.J. Smith, Appl. Catal. A 328 (2007) 58–67.
[36] A. Infantes-Molina, J. Mérida-Robles, E. Rodríguez-Castellón, J.L.G. Fierro, A. Jiménez-López, Appl. Catal. B 73 (2007) 180–192.
[37] A. Bertrand, J. Vac. Sci. Technol. 18 (1981) 28–33.
[38] P.E.R. Blanchard, A.P. Grosvenor, R.G. Cavell, A. Mar, Chem. Mater. 20 (2008) 7081–7088.
[39] D.J. Sicinolfi, R.P. Frankenthal, J. Electrochem. Soc. 136 (1989) 2475–2480.
[40] S.T. Oyama, Y.-K. Lee, J. Catal. 258 (2008) 393–400.
[41] J.A. Cecilia, et al. Appl. Catal. B: Environ 92 (2009) 100–113.
[42] S.L. Brock, K. Senevirathne, J. Solid State Chem. 181 (2008) 1552–1559.
[43] Y.-K. Lee, S.T. Oyama, J. Catal. 239 (2006) 376–389.